Structure conformational and rheological characterisation of alfalfa seed (Medicago sativa L.) galactomannan

Thierry Hellebois, Christos Soukoulis, Xuan Xu, Jean-Francois Hausman, Alexander Shaplov, Petros Taoukis, Claire Gaiani

Carbohydrate Polymers 256 (2021) 117394

Contents lists available at ScienceDirect

Carbohydrate Polymers

journal homepage: www.elsevier.com/locate/carbpol

Structure conformational and rheological characterisation of alfalfa seed (*Medicago sativa* L.) galactomannan

Thierry Hellebois [a,b], Christos Soukoulis [a,*], Xuan Xu [a], Jean-Francois Hausman [a], Alexander Shaplov [d], Petros S. Taoukis [c], Claire Gaiani [b]

[a] Environmental Research and Innovation (ERIN) Department, Luxembourg Institute of Science and Technology (LIST), 5 avenue des Hauts Fourneaux, L4362, Esch-sur-Alzette, Luxembourg
[b] Université de Lorraine, LIBio, Nancy, France
[c] Laboratory of Food Chemistry and Technology, School of Chemical Engineering, National Technical University of Athens, 15780, 5 Iroon Polytechniou Str., Athens, Greece
[d] Materials Research and Technology (MRT) Department, Luxembourg Institute of Science and Technology (LIST), 5 avenue des Hauts Fourneaux, L4362, Esch-sur-Alzette, Luxembourg

ARTICLE INFO

Keywords:
Lucerne
Galactomannan
Viscoelasticity
Flow behaviour
Intrinsic viscosity
Molecular weight
Oscillatory thermo-rheology

ABSTRACT

In the present work a galactomannan extract of low protein residue (< 1.3 % wt dry basis) was isolated from alfalfa (*Medicago sativa* L.) seed endosperm meal. The alfalfa gum (AAG) comprised primarily mannose and galactose at a ratio of 1.18:1, had a molecular weight of 2×10^6 Da and a radius of gyration of 48.7 nm. The average intrinsic viscosity of the dilute AAG dispersions calculated using the modified Mark-Houwink, Huggins and Kraemer equations was 9.33 dLg^{-1} at 25 °C. The critical overlap concentration was estimated at 0.306 % whereas the concentration dependence of specific viscosity for the dilute and semi-dilute regimes was $\propto C^{2.3}$ and $C^{4.2}$, respectively. The compliance to the Cox-Merz rule was satisfied at 1% of AAG, whereas a departure from superimposition was observed at higher concentrations. Viscoelasticity measurements demonstrated that AAG dispersions exhibit a predominant viscous character at 1 % wt, whereas a weak gel-like behaviour was reached at AAG concentrations ≥3 %.

1. Introduction

Market globalisation, emerging issues associated with food security and sustainable management of food biomass and natural resources concern a major challenge for food ingredient manufacturers. Carbohydrate food biopolymers i.e. polysaccharides and oligosaccharides constitute a major group of food ingredients due to their multifaceted techno-functionality and important role as dietary and biologically active macromolecules (Williams & Phillips, 2009). In the last decade, the attempts to valorise food industry side-streams or underexploited food biomass as alternative sources of food and nutraceutical relevant carbohydrate polymers are steadily gaining popularity. In this context, different food industry side-streams including cereals, legumes, oilseed crops, vegetable and fruit residues, plant cladodes etc. have been evaluated for their potential to provide marketable solutions in the domain of food biomacromolecules (Ben-Othman, Jõudu, & Bhat, 2020; Soukoulis, Gaiani, & Hoffmann, 2018).

Galactomannans are heterogeneous polysaccharides comprising a β-(1→4) D-mannose backbone branched with α-(1→6) linked D-galactose monomeric units. It is well established that the mannose to galactose (M/G) ratio varies with the their botanical origin and modulates their techno-functional properties i.e. cold-water swelling ability, thickening, gelling, film forming and cryogelation properties (Kontogiorgos, 2019). The commercially available galactomannans (on approximate increasing M/G ratio) include fenugreek (1:1, *Trigonella foenum-graecum* L.), guar (2:1, *Cyamopsis tetragonoloba*), tara gum (3:1, *Caesalpinia spinosa*), locust bean gum (4:1, *Ceratonia siliqua*) and cassia gum (5:1, *Cassia tora*) (Prajapati et al., 2013). In addition, galactomannans from underexploited plant seed sources such as honey locust (*Gleditsia triacanthos*), Chinese locust (*Gleditsia sinensis*), clover (*Melilotus albus* and *Melilotus officinalis*), flame tree (*Delonix regia*), yellow flame tree (Peltophorum pterocarpum), creamy peacock flower (*Delonix elata*), mesquite (*Prosopsis juliflora*), henna (*Cassia fistula*), and malu creeper (*Bauhinia vahlii*) have been successfully isolated and

* Corresponding author.
E-mail address: christos.soukoulis@list.lu (C. Soukoulis).

https://doi.org/10.1016/j.carbpol.2020.117394
Received 22 September 2020; Received in revised form 3 November 2020; Accepted 8 November 2020
Available online 11 November 2020

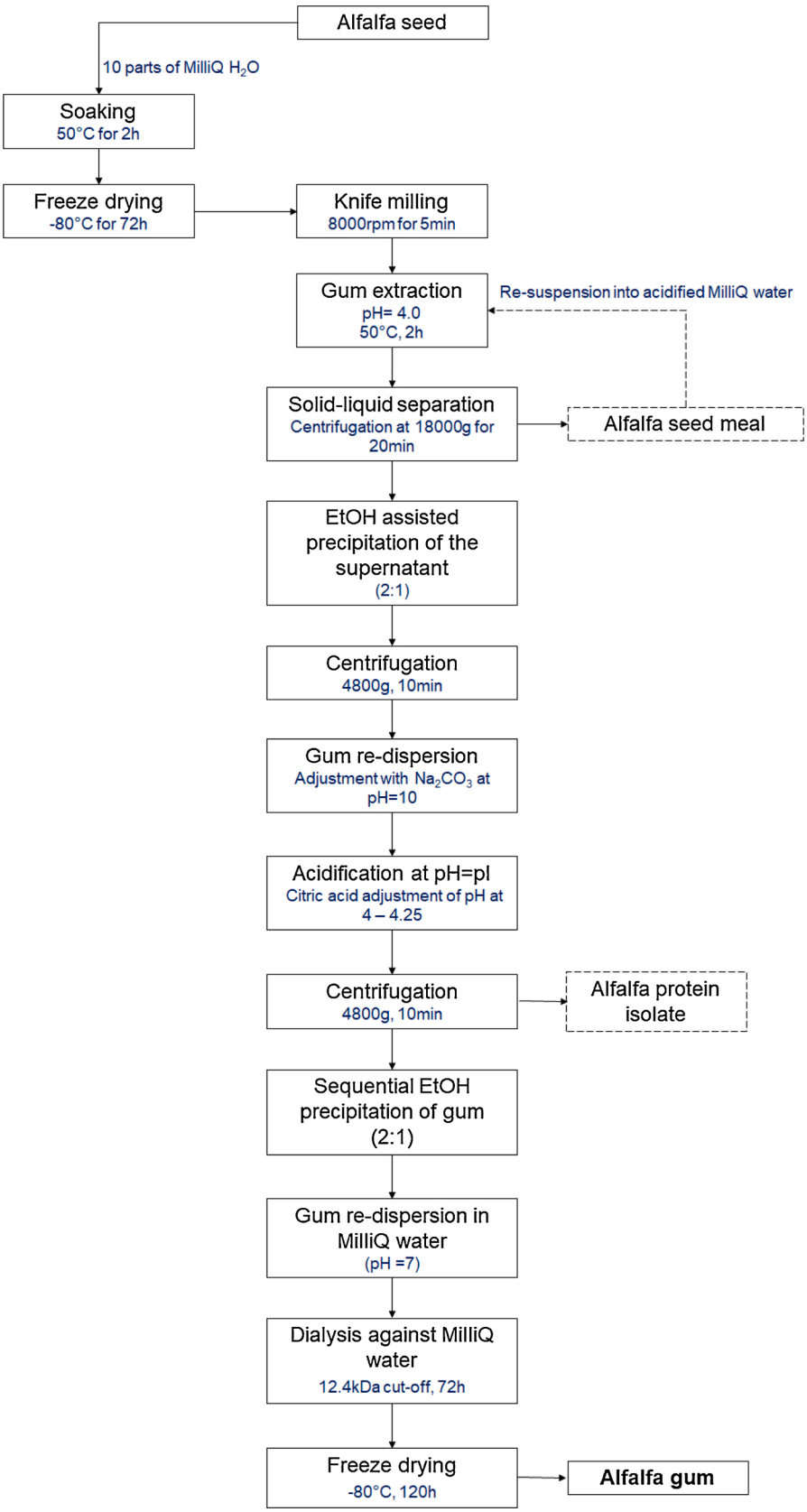

Fig. 1. Illustration of the clean label methodology adopted for extracting and purifying the galactomannan from the endosperm of alfalfa seeds.

characterised (Jamir, Badithi, Venumadhav, & Seshagirirao, 2019; Liu, Xu, Lei, Li, & Jiang, 2019; López-Franco, Cervantes-Montaño, Martínez-Robinson, Lizardi-Mendoza, & Robles-Ozuna, 2013; Rodriguez-Canto, Chel-Guerrero, Fernandez, & Aguilar-Vega, 2019; Sciarini, Maldonado, Ribotta, Pérez, & León, 2009). Recently, spent coffee grounds have been reported as a promising bioresource for exploiting galactomannan and arabinogalactan rich fractions (Moreira, Nunes, Domingues, & Coimbra, 2015).

Alfalfa (*Medicago sativa* L.) is a perennial herbaceous forage legume cultivated world-wide due to its high nutritional value as fodder and feed for livestock. Alfalfa is also recognised for its sustainable character, excellent adaptability to extreme climate conditions, and ecological resilience e.g., alfalfa assists in soil protection, nitrogen fixation, mitigation of soil contaminants, lowering of air contaminants, carbon dioxide sequestration etc (Bacenetti, Lovarelli, Tedesco, Pretolani, & Ferrante, 2018). From an economical viewpoint, combined alfalfa exploitation (forage and seeds) can significantly improve several economic indices including gross margin, cost effectiveness quotient, and profit rate (Boelt, Julier, Karagić, & Hampton, 2015; Pajić & Marković, 2016). In the framework of actions for counteracting food security issues, alfalfa leaf meal has received much attention in the last years. It has been previously reported that alfalfa leaf meal contains at least 20 % proteinaceous matter of similar essential amino acid composition to that of soybean protein concentrate, and 17–27 % of soluble and insoluble dietary fibres (Hojilla-Evangelista, Selling, Hatfield, & Digman, 2017; Mielmann, 2013). In addition, a plethora of micronutrients including carotenoids, tocopherol, polyphenols, saponins and vitamins of the B-complex have been identified (Cornara, Xiao, & Burlando, 2016; Mielmann, 2013). In regard to the polysaccharides profile of alfalfa forage, it has been shown that the total polysaccharides content and the sugar monomers composition are dependent on the extraction and fractionation conditions (Wang, Dong, Ma, Cui, & Tong, 2014; Wang, Dong, & Tong, 2013). Wang et al. (2014) demonstrated that polysaccharide fractions of 20–60 kDa containing ca. 37–52 % of uronic acids could be obtained via ion-exchange and size-exclusion chromatography. All polysaccharide fractions exerted a dose dependant (up to 1000 μg mL^{-1}) protective effect against hydrogen peroxide induced oxidative stress, whereas the hepatotoxicity levels were minimised when fractions of high uronic content and molecular weight were administered to the hepatocytes in-vitro model. In two consecutive studies Chen, Liu, Zhang, Dai et al. (2015) and Chen, Liu, Zhang, Niu et al. (2015) investigated the techno-functionality and bioactivity of the hemicellulosic and pectic polysaccharide fractions isolated from hot alkali extracts of alfalfa stems. Despite the differences in their structure conformational profile, both polysaccharide fractions exerted good thermal stability and significant suppression effects on pro-inflammatory cytokine genes such as IL-1β, IL-6 and COX-2.

Rudimentary studies of alfalfa seed compositions reported that the major polysaccharide component of alfalfa seeds belongs in the galactomannan class (Dobrenz, Smith, Poteet, & Miller, 1993; Grasdalen & Painter, 1980; McCleary & Matheson, 1975). Nonetheless, the structure conformational and technological aspects of the alfalfa galactomannans remain poorly studied. This study aimed at the extraction, purification and assessment of the structure conformational, steady, dynamic and thermo-rheological properties of galactomannan from the endosperm of alfalfa seeds.

2. Materials and methods

2.1. Materials

Organic alfalfa seeds (Food to Live, New York, USA) were purchased from the local market. All organic solvents and chemicals used for the extraction and the analysis of the alfalfa gum were of analytical grade and obtained from Sigma-Aldrich (Leuven, Belgium).

2.2. Extraction and isolation of the alfalfa gum

A schematic representation of the method used for the extraction and isolation of alfalfa gum is given in Fig. 1. In specific, alfalfa seeds were soaked in MilliQ water (pH = 4 using 0.5 % w/w citric acid), Millipore Inc., US) at 50 °C for 2 h under mild magnetic stirring (IKA GmbH, Staufen, Germany). To facilitate the hydration of the seeds, the alfalfa seed to water ratio was maintained at 1:10 (w/w). The alfalfa seed suspension was vacuum filtered using a Buchner funnel with fritted disc and the obtained seed solids were freeze dried at −80 °C for 72 h (Alpha 2–4 LSCplus, Christ, Osterode am Harz, Germany). The lyophilised seeds were ground (8,000 rpm for 5 min) using a knife mill (Grindomix GM300, Retsch, Haan, Germany) and the obtained alfalfa meal was mixed with MilliQ water at a 1:50 (w/w) ratio and kept at 50 °C under mechanical stirring for 2 h to allow sufficient extraction of the water soluble biopolymers.

Then, the alfalfa meal suspension was centrifuged at 18,000 *g* for 15 min and the supernatants obtained after two consecutive washings of the alfalfa solids (with Milli-Q water at 1:10 ratio) were pooled and mixed (1:2) with anhydrous ethanol to promote aggregation and precipitation of the polysaccharides. The ethanolic suspension was centrifuged at 4,800 *g* for 10 min and the obtained gum pellets were flashed with nitrogen to evaporate the ethanol excess and reconstituted in MilliQ water adjusted with sodium carbonate at pH = 10 and kept under stirring at 50 °C until complete dissolution of the gum solids. To remove the protein impurities, the pH of the biopolymer solution was adjusted at the isoelectric point of alfalfa proteins (i.e. pI ≈ 4–4.25) using citric acid. The resulting suspension was centrifuged at 18,000 *g* for 15 min and the supernatant was neutralised (pH = 7) using sodium carbonate. For removing the residual sodium citrate, the polysaccharide solution was dialysed (cut-off 12.4 kDa) against MilliQ water for 72 h. Finally, the dialysed polysaccharide aliquots were freeze dried at −80 °C for 5 days (Alpha 2–4 LSCplus, Christ, Germany), and the obtained gum lyophilisates were stored under controlled temperature and relative humidity conditions (a_w = 0.11, 25 °C). For comparison purposes, galactomannans were also extracted from defatted fenugreek seed meal (*Trigonella foenum-graecum*, Arkopharma, Belgium) following the aforementioned procedure.

2.3. Compositional and structure conformational properties determination

2.3.1. Proximate composition analysis

Moisture and ash content of the galactomannan gum extracts were gravimetrically determined according to the AOAC standard methods. The protein content was determined according to the Dumas method using a CHNS analyser (Elementar Vario Cube, Langensenbold, Germany). Total carbohydrate content was determined using an enzymatic assay kit (Megazyme, K-ACHDF 08/16). Total lipid content was determined by difference.

2.3.2. Sugar monomer and uronic acid composition analysis

The sugar monomer composition of the galactomannan gum extracts was determined according to the method of Qian, Cui, Wu, and Goff (2012) with minor modifications. In brief, 20 mg of the galactomannan were transferred into an Eppendorf tube with screw cap, mixed with 1 mL of sulphuric acid 2 M and incubated at 99 °C with intermittent stirring for 4 h using a Thermomixer (Thermomixer R, Eppendorf, Germany). On completion of incubation, the tubes were cooled down in an ice bath, centrifuged at 10,000 *g* for 5 min and the supernatants were carefully collected using a syringe. The sample preparation was carried out in four replicates.

The hydrolysate was diluted 1:300 and 1:500 with MilliQ water and analysed using a Dionex™ ICS-5000+ Capillary HPIC™ System coupled with a pulsed electrochemical detector (Thermo Scientific™ Dionex™). The separation of monosaccharides was performed with a CarboPac

SA10 analytic column (2 × 250 mm, Thermo Scientific™ Dionex™) and a CarboPac PA20 analytic column (3 × 150 mm, Thermo Scientific™ Dionex™). For SA10 column, 100% 1 mM NaOH was used as an eluent to separate the monosaccharide at a constant flow rate of 0.38 ml min^{-1} at 45 °C. For the PA20 column, the separation of monosaccharides was performed using 4 % 1 mM NaOH at a flow rate of 0.5 ml min^{-1} at 30 °C. The retention time obtained with a single injection of each standard was used to identify each monosaccharide. The quantification of monosaccharides was performed using a calibration curve generated with varying standard concentrations (1, 2.5, 5, 7.5, 10, 25, 50, 75 and 100 μmol L^{-1}). Data acquisition and analysis were carried out using Chromeleon™ Chromatography Data System Software (Thermo Scientific™).

2.3.3. Gel permeation size-exclusion chromatography (GPC/SEC)

A 1200 Infinity gel permeation chromatograph (GPC, Agilent Technologies) was used to determine M_n, M_w, M_z and M_w/M_n of the polymers. The chromatograph was equipped with an integrated IR detector, two columns (PL aquagel-OH MIXED-H and PL aquagel-OH MIXED-M) and a PL aquagel-OH guard column (Agilent Technologies). 0.1 M $NaNO_3$ aqueous solution containing 0.02 % (w/v) of NaN_3 was used as an eluent, the flow rate was maintained at 1.0 mL $min^{-1}$and the measurements were performed at 50 °C. Pullulan standards (ReadyCal-Kit Pullulan high, PSS Polymer Standards Service GmbH, M_p = 180–1,530 × 10^3) were used to perform calibration. All the samples were filtered through a 0.2 μm Teflon filter prior injection.

The Flory-Fox model (Eq. (1)) was used to calculate the radius of gyration (R_g) as follows:

$$R_g = \left[\frac{[\eta]\overline{M_w}}{\Phi_0}\right]^{1/3} \quad (1)$$

where Φ_0 is a proportionality constant equal to 2.86 × 10^{23} mol^{-1} for random coil and linear polysaccharides (Gillet et al., 2017).

The number-average degree of polymerisation of the gum (DP_n) was calculated as follows:

$$DP_n = \frac{M_n}{M_0} \quad (2)$$

where M_n is the number-average molecular weight of the polymer and M_0 the molecular weight of the repeating unit.

2.4. Intrinsic viscosity measurements

The intrinsic viscosity [η] of dilute alfalfa gum dispersions (0.01–0.1 % wt) in MilliQ water was measured using 0C Ubbelohde capillary viscometer (Paragon Scientific, United Kingdom) at 25 ± 0.1 °C. The intrinsic viscosity was determined as the intercepts of the Huggins (Eq. (3)) and Kraemer (Eq. (4)) equations by extrapolating to an infinite dilute system:

$$\frac{\eta_{sp}}{C} = [\eta] + k_H[\eta]^2 C \quad (3)$$

$$\frac{\ln\eta_{rel}}{C} = [\eta] + k_K[\eta]^2 C \quad (4)$$

where: η_{sp} and η_{rel} denote the specific and relative viscosity, respectively, C is the alfalfa gum concentration, and k_H and k_K are the Huggins and Kraemer coefficients, respectively.

2.5. Steady state and dynamic rheological measurements

Aqueous dispersions (0.1, 0.25, 0.5, 0.75, 1, 2, 3, and 4 % wt) of alfalfa gum in MilliQ water (adjusted at pH = 7 using NaOH 0.1 M) were prepared for conducting the rheological measurements. All rheological measurements were performed in an Anton-Paar oscillatory rheometer (MCR 302, Graz, Austria) equipped with either a concentric cylinder (steady state rheological measurements) or cone plate geometry (dynamic rheological measurements).

2.5.1. Flow behaviour

Aliquots of the galactomannan dispersions (*ca.* 15 mL) were transferred to the measuring geometry and tempered at ambient temperature (25 ± 0.05°C) for 20 min prior to the analyses. Due to the time-dependent flow behaviour of the solutions, a pre-shearing (at 200 s^{-1} for 5 min) of the gum dispersions was applied until a steady state to be achieved. Upward shear rate sweeps in the range of 1 to 1,000 s^{-1} were performed. The obtained shear stress τ (Pa) – shear rate $\dot{\gamma}$ (s^{-1}) data were fitted into the Ostwald-de Waele (Power) model (Eq. (5)) as follows:

$$\tau = K\ \dot{\gamma}^n \quad (5)$$

where K (Pa s^{-n}), n, τ_0 (Pa) and η_∞ (Pa s) denote the consistency coefficient, rheological behaviour index, yield stress and limiting viscosity at infinite shear rate, respectively.

2.5.2. Zero shear viscosity measurements

To determine the critical concentration of alfalfa gum, the limiting viscosity at zero shear rate (η_0) was determined for galactomannan gum aqueous dispersions in the concentration range of 0.1–2 % w/w. For this purpose, the Williamson-Cross model (Eq. (6)), was fitted into the obtained viscosity – shear rate (0.01 to 1,000 s^{-1}) data:

$$\eta = \eta_\infty + \frac{\eta_0 - \eta_\infty}{1 + C\cdot\dot{\gamma}^m} \quad (6)$$

where η_0 and η_∞ represent the zero and infinite shear viscosity, and C, m are the Cross time and rate constants, respectively.

2.5.3. Amplitude and frequency sweep measurements

For the dynamic rheological measurements, alfalfa gum dispersions in the concentration range of 1–4% w/w were prepared. Amplitude sweeps were conducted to determine the linear viscoelastic region (LVR) under controlled shear stress conditions, at 1 Hz and 25 °C. From the obtained amplitude sweep rheological spectra, the viscoelastic moduli and stiffness (G'_{LVR} and G''_{LVR}, $\tan\delta_{LVR}$) in the LVR regime, the yield stress at the limit of LVR regime (τ_y) and the strain and stress flow-point ($G' = G''$) were calculated using the RheoCompass analysis software (Anton-Paar, Graz, Austria).

Frequency sweeps (0.1–100 Hz) within the LVR regime (strain = 0.5 %) were performed at 25 °C to evaluate the viscoelastic profile of the alfalfa gum dispersions. The slope of the double logarithmic storage modulus (G′) – angular frequency (ω) curves was calculated. In addition, the frequency (f) at the which the crossover of the viscoelastic moduli ($G' = G''$) takes place was calculated using Solver (Excel, Microsoft Inc).

2.6. Oscillatory thermo-rheology (OTR) and determination of non-isothermal kinetic parameters

For the OTR measurements, the alfalfa gum dispersions were heated from 25 to 70 °C at the rate of 5 °C min^{-1} and kept isothermally for 10 min. A small amount of silicon oil was carefully applied on the cone-plate edge surface to prevent water evaporation. Monitoring of storage (G′) and loss moduli (G″) as well as complex viscosity (η*) was conducted within the LVE regime (strain: 1 %, frequency: 1 Hz). The following temperature ramp protocol was implemented: a) cooling from 70 to 5 °C at the rate of 2 °C·min^{-1}, b) isothermal holding at 5 °C for 10 min and c) heating from 5 to 70 °C at the rate of 2 °C min^{-1}. The temperature points, where the viscoelastic crossover ($G' = G''$) occurs, were recorded.

It was previously shown (Razavi, Alghooneh, & Behrouzian, 2018) that the temperature dependence of rheological parameters on heating

Table 1
Proximate and sugar monomer compositional properties of the alfalfa, fenugreek, guar and locust bean gums.

	Alfalfa gum	Fenugreek gum	Guar gum	Locust bean gum
Proximate composition[1]				
Total carbohydrates (%)	96.7 ± 1.2bc	97.1 ± 0.4c	95.2 ± 0.1b	92.9 ± 0.2a
Protein (%)	1.3 ± 0.1a	1.3 ± 0.3a	3.9 ± 0.1b	6.0 ± 0.3c
Ash (%)	2.0 ± 0.2c	1.6 ± 0.4c	0.9 ± 0.01a	1.1 ± 0.01b
Sugar monomers composition (g/100 g of total carbohydrate matter)				
Arabinose	0.20 ± 0.0a	0.7 ± 0.0b	1.4 ± 0.1c	1.2 ± 0.1c
Galactose	46.0 ± 2.8c	44.1 ± 0.9c	33.0 ± 2.1b	25.2 ± 1.5a
Glucose	0.30 ± 0.0b	0.2 ± 0.0a	1.2 ± 0.1c	2.0 ± 0.1d
Mannose	53.8 ± 3.0a	55.1 ± 0.2a	64.3 ± 3.9b	71.6 ± 2.1c
Fucose	nd	nd	nd	nd
Rhamnose	nd	nd	0.1 ± 0.0	nd
Uronic acids	nd	nd	nd	nd
M/G	1.18 ± 0.14a	1.24 ± 0.08a	2.00 ± 0.24b	2.74 ± 0.09c

[a–d] Different letters between the rows indicate significant difference ($p < 0.05$) according to Tukey's post hoc means comparison test.
[1] Calculated on dry basis; lipid matter was detected in traces.

or cooling cycles can be described by three main equations: the rate of reaction (Eq. (7)), the Arrhenius equation (Eq. (8)) and the time-temperature relationship (Eq. (9)).

$$\frac{d\eta^*}{dt} = k\cdot\eta^{*n} \tag{7}$$

where η^* is the complex viscosity (in Pa·s), and n is the order of the viscosity change kinetics.

$$k = k_0(Tref)\cdot\exp\left(-\frac{E_a}{R(T-Tref)}\right) \tag{8}$$

where k_0 is the pre-exponential factor, R the universal gas constant (R = 8.314 $Jmol^{-1}K^{-1}$), T the temperature (°K) and E_a the activation energy ($J\ mol^{-1}$)

$$T = T_0 + \lambda\cdot t \tag{9}$$

where, T_0 is the initial temperature (i.e. 70 or 5 °C for cooling and heating profiles) and λ the cooling or heating rate (i.e. 2 °C min^{-1}).

Using the Arrhenius equation, the Eq. (7) can be re-written as follows:

$$\frac{d\eta^*}{dt} = k_0(Tref)\cdot\exp\left(-\frac{E_a}{R(T\text{-}Tref)}\right)\cdot\eta^{*n} \tag{10}$$

which by logarithmic transformation yields:

$$\ln\left(\frac{d\eta^*}{dt}\right) - \ln(\eta^{*n}) = \ln k_0(Tref) - \frac{E_a}{R(T-Tref)} \tag{11}$$

Derivation of Eq. (9) gives:

$$dT = \lambda\cdot dt \tag{12}$$

Considering that the data were best fitting to second-order kinetics i.e. $n = 2$ and taking into account the Eqs. (10) and (11), it is obtained:

$$\ln\left(\lambda\frac{d\eta^*}{dT}\times\frac{1}{\eta^2_*}\right) = \ln k_0(Tref) - \frac{E_a}{R(T\text{-}Tref)} \tag{13}$$

For the calculation of the kinetic parameters i.e. k_0 and E_a, the $\frac{d\eta^*}{dT}$ parameter was determined by deriving a low order polynomial model fitting the elastic modulus – temperature data:

$$\frac{d\eta^*(T)}{dT} = \frac{d\left(a_mT^m + a_{m\text{-}1}T^{m-1} + \ldots + a_1T^1 + a_0\right)}{dT} \text{ with } m \le 3 \tag{14}$$

The adopted approach for calculating the $\frac{d\eta^*}{dT}$ was also pre-validated numerically to ensure sufficient accuracy in the estimation of the kinetic parameters.

2.7. Statistical analyses

The normal distribution of the data was verified by means of the Shapiro-Wilk test and Q-Q plot representation. In addition, the equality of variance among the variables was verified using the Levene's test. To determine the significance of the alfalfa gum concentration on the physicochemical and rheological properties, one-way ANOVA was performed using SPSS software (IBM, USA). Tukey's multiple range test was used to separate means of data when significant differences ($p < 0.05$) were detected.

3. Results and discussion

3.1. Proximate and sugar monomers composition

For comparison purposes, the compositional profile of alfalfa gum was contrasted to that of in-house extracted fenugreek gum as well as commercially available guar and locust bean gums. It is well established that the yield and compositional profile of plant seed extracts are influenced by several parameters including the botanical origin and cultivar type of the plant seed, the extraction conditions (temperature, seed to solvent mass ratio, pH and ionic strength) as well as the gum purification treatments (Soukoulis et al., 2018). The yield of the extraction for the alfalfa gum was estimated at 20.53 ± 0.22 %, whereas following the same extraction protocol, the yield for fenugreek gum was determined at 27.0 ± 2.1 %. As seen in Table 1, alfalfa gum was composed of 96.7 % total carbohydrates, 1.3 % protein, 2.0 % ash and <

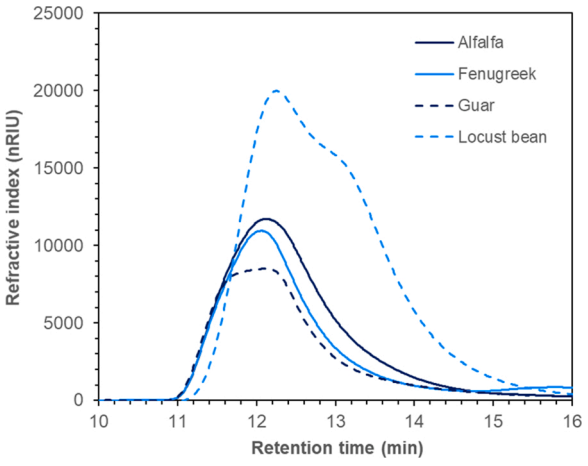

Fig. 2. Gel permeation size-exclusion chromatogram (GPC/SEC) of commercial (dotted lines) and in-house extracted (straight lines) galactomannan gums.

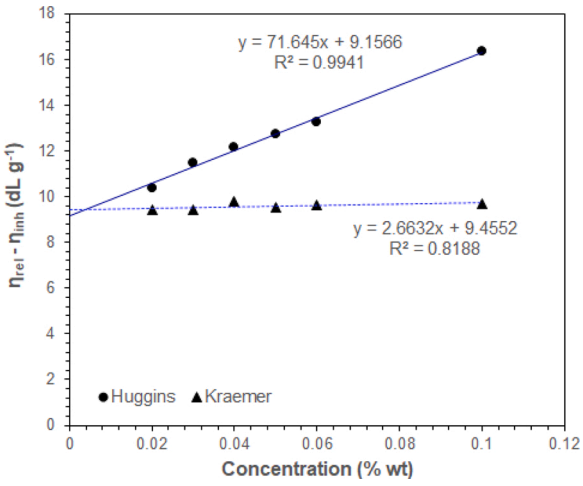

Fig. 3. Inherent (Kraemer) and relative (Huggins) viscosity as a function of alfalfa gum concentration at 25 °C.

0.1 % lipids residual matter (on dry basis). Interestingly, both alfalfa and fenugreek gum extracts were characterised by a notably low protein residue (protein content in the commercial galactomannans was 3.9 and 6.0 % w/w for guar and locust bean gum, respectively), suggesting that the acid-assisted extraction and the isoelectric protein precipitation steps concomitantly resulted in a significantly lower amount of protein impurities in the purified gum extract. Galactomannans can be further stripped of their protein impurities via either enzymatic (proteases) or organic-solvent (e.g. isopropanol or biphasic phenol-water system) assisted deproteinisation treatments.

In terms of sugar monomers composition (Table 1), alfalfa gum was primarily composed of mannose (M) and galactose (G) sugar moieties at a M/G ratio of 1.18, whilst substantially lower amounts of other sugars such as arabinose and glucose were also detected. As expected, alfalfa gum exhibited an almost identical sugar composition profile to that of fenugreek gum obtained following the same extraction procedure (M/G = 1.24), whilst significantly higher M/G ratios were observed in the case of guar and locust bean gums i.e. 2.00 and 2.74, respectively. Our observations corroborate the literature data for alfalfa (M/G 1.09–1.28), fenugreek (M/G 1.05–1.26), guar gum i.e. M/G 1.65–2.00 and locust bean gum i.e. M/G 3.00–3.70 (Bourbon et al., 2010; Dhull et al., 2020; Grasdalen & Painter, 1980; Liu, Lei, He, Xu, & Jiang, 2020; Wu, Cui, Eskin, & Goff, 2009).

3.2. Structure conformation molecular properties

The GPC/SEC chromatographs of alfalfa, fenugreek, guar and locust bean gum are shown in Fig. 2. Contrary to locust bean gum, alfalfa, fenugreek and guar gum exhibited a monomodal (less pronounced for guar gum) size distribution with a long tail towards the lower molecular weight. The molecular weight of alfalfa gum was calculated as 2.00 × 10^6 Da, which was almost identical to that fenugreek gum extracted with the same procedure (2.02 × 10^6 Da) and lower than the M_w of the commercial guar gum (2.31 × 10^6 Da).

It is well established that the M_w of galactomannans can be highly diversified by parameters such as their botanical and geographical origin, the extraction and fractionation conditions (e.g. pH, temperature, type of organic solvents used for aggregation), the extent of the galactosyl substitution or depolymerisation etc (Mathur, 2016). It is also worth noting that the presence of protein impurities in the gum extract could modify significantly the average molecular weight of the gum. Youssef, Wang, Cui, and Barbut (2009) reported an increase in fenugreek gum molecular weight from 1.46 × 10^6 to 2.28 × 10^6 Da by reducing the protein content from 3.7% to 1.1 %, respectively. In this context, M_w of alfalfa gum was found to be in range with other galactomannans having a M/G ratio of ~ 1.0, such as fenugreek (from 0.56× 10^6 to 2.35 × 10^6 Da) (Brummer, Cui, & Wang, 2003; Wei et al., 2015; Youssef et al., 2009).

The intrinsic viscosity [η] of the alfalfa gum dispersions was experimentally determined in the dilute regime i.e. $1.2 < \eta_{rel} < 2.0$ and C < 0.1% wt using the Huggins and Kraemer equations (Fig. 3). For comparison purposes, the [η] of all galactomannans was also determined using the Mark-Houwink equation as modified by Doublier and Launay (1981) for aqueous galactomannan dispersions (Eq. 15):

$$[\eta] = 11.55 \cdot 10^{-6} \left(\left(1 - \frac{G}{(G+M)} \right) \cdot \overline{M_w} \right)^{0.98} \quad (15)$$

where G and M denote the mass fractions for galactose and mannose sugar monomers and $\overline{M_w}$ is the polymer weight average molecular weight obtained from GPC/SEC analysis. As illustrated in Fig. 3, the [η] of alfalfa gum was determined at 9.16 and 9.45 dL g^{-1} according to Huggins and Kraemer equations, respectively, whilst it was estimated at 9.40 dL g^{-1}using the modified Mark-Houwink equation (Table 2). Thus, there is practically no discrepancy between the value of [η] obtained from GPC experiments carried out at 50 °C and the intrinsic viscosity calculated using the MKHS coefficients obtained at a different temperature (25 °C). In turn, this suggests that the volume occupied by macromolecules in solution was not depend strongly on temperature. The [η] values for the rest galactomannans were estimated at 9.04, 12.87 and 7.86 dL g^{-1} for fenugreek, guar and locust bean gum, respectively. Therefore, it can be deduced that the Huggins-derived [η] of alfalfa gum is in range with that reported for other galactomannans of ~ 1.0 M/G ratio, such as fenugreek gum (9.1–13.6 dL g^{-1}) and *Mimosa scabrella* (9.0 dL g^{-1}), and lower than guar gum (9.1–17.2 dL g^{-1}) (Cheng, Brown, & Prud'homme, 2002; Doublier & Launay, 1981; Gadkari, Tu, Chiyarda,

Table 2
Comparison of structure conformational characteristics of different galactomannans. Alfalfa and fenugreek gums were extracted adopting the herein reported method whilst guar and locust bean gums were of commercial grade.

	Alfalfa gum	Fenugreek gum	Guar gum	Locust bean gum
$\overline{Mn}$ (×10^5 Da)	10.21 ± 0.75b	12.85 ± 0.98c	12.86 ± 1.5c	5.5 ± 0.55a
$\overline{Mw}$ (×10^5 Da)	19.96 ± 1.92b	20.19 ± 0.85b	23.11 ± 2.18b	12.12 ± 0.36a
$\overline{Mz}$ (×10^5 Da)	28.49 ± 1.4b	27.39 ± 1.08b	31.08 ± 1.77b	18.78 ± 0.29a
Đ	2.11 ± 0.34bc	1.57 ± 0.11a	1.85 ± 0.19b	2.20 ± 0.12c
$\overline{DP}_n$	5667 ± 416b	7138 ± 544c	7140 ± 833c	3053 ± 305a
[η] (dL g^{-1})	9.33 ± 0.3b	9.04 ± 0.3b	12.87 ± 0.3c	7.86 ± 0.1a
R_g (nm)	40.7 ± 0.22b	40.5 ± 0.18b	47.6 ± 0.31c	32.6 ± 0.17a
z-diameter (nm)	97.6 ± 4.2b	65.5 ± 3.9a	75.1 ± 5.1a	128.6 ± 9.8c

[a–d] Different letters between the rows indicate significant difference ($p < 0.05$) according to Tukey's post hoc means comparison test. Symbol used: number average molecular weight (Mn), weight average molecular weight (Mw), z-average molecular weight (Mz), polydispersity index (Đ), number-average degree of polymerisation (DP_n), intrinsic viscosity ([η]), radius of gyration (R_g).

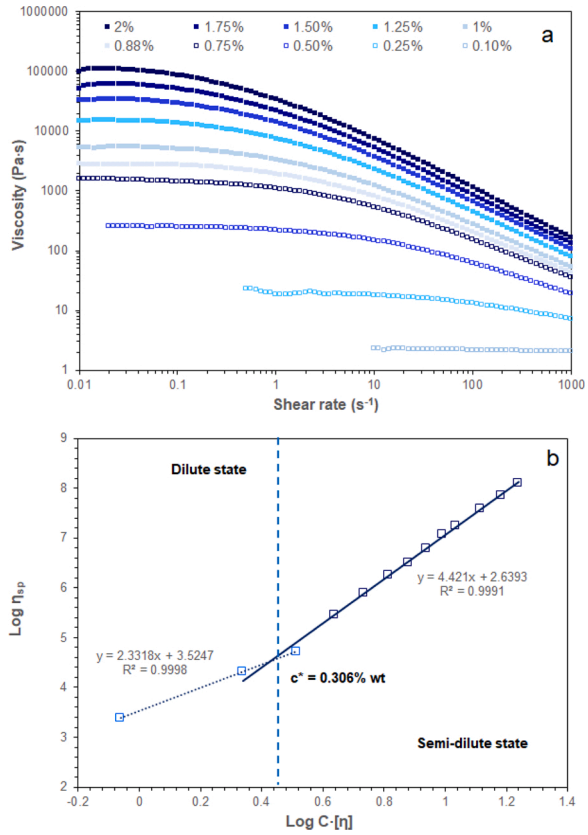

Fig. 4. Flow behaviour curves of alfalfa gum dispersion as influenced by gum concentration (a); double logarithmic plot of specific viscosity at zero shear rate ($\eta_{sp,0}$) as a function of coil overlap parameter C[η] for alfalfa gum dispersions at 25 °C (b).

Table 3
Steady flow characteristics of alfalfa gum dispersions (0.5 to 4% w/w) as calculated according to Ostwald-de Waele, and Williamson models.

Gum concentration	Ostwald – de Waele model		Cross-Williamson model		
	K (Pa s^{-n})	n	τ (s)	$\dot{\gamma}_{crit}$ (s^{-1})	m
0.1	–	–	–	–	–
0.25	0.031	0.811	0.006	150.5	0.407
0.5	0.511	0.562	0.059	16.9	0.642
0.75	1.85	0.445	0.302	3.32	0.642
1.0	5.63	0.351	0.582	1.72	0.736
1.25	11.8	0.295	1.16	0.865	0.750
1.5	21.4	0.253	1.79	0.558	0.779
1.75	32.0	0.226	2.21	0.453	0.827
2.0	47.1	0.207	3.05	0.328	0.831

Reaney, & Ghosh, 2018; Ganter, Milas, Corrêa, Reicher, & Rinaudo, 1992; Gillet et al., 2017; Liu et al., 2020).

The [η] provides a proximate estimation of the size and structure molecular conformation of the polymer chains in a given solvent. The Huggins and Kraemer constants k_H and k_K for alfalfa gum were 0.85 and 0.02, respectively, indicating a rather poor solvent (deionised water) affinity that favours the self-association (aggregation) of the polymer chains. In general, a good polymer solvation is achieved when $0.25 < k_H < 0.5$ and $k_K < 0$ (Marani, Hjelm, & Wandel, 2013). The obtained k_H and k_K values for alfalfa gum, are higher than the literature reported for fenugreek gum ($k_K = -0.07$) albeit their M_w and M/G ratio similarities (Gadkari et al., 2018). Nonetheless, the k_H and k_K values for alfalfa gum remain significantly lower than those reported for galactomannans of remarkably different chemical structure conformation such as guar, locust bean and tara gum. Gillet et al. (2017) ascribed the disparities in the k_H and k_K values to differences in the polymer chains length and distribution of galactosyl groups (resulting in localised hydrophobic patches), which are induced by the gum extraction and/or fractionation conditions.

Comparing the radii of gyration (R_g) data obtained using either the Fox-Flory equation or experimentally by means of dynamic light scattering (Table 2), discrepancies between the measured and predicted values were found. The Flory Fox equation resulted in underestimated R_g values for all galactomannans, most probably due to the occurrence of associative aggregation. Interestingly, galactomannans having identical M/G ratio and Mw, did not exhibit the same hydrodynamic volume occupancy ($\langle R_g \rangle_z$ was larger in the case of alfalfa gum), which supports the hypothesis that the polymer – solvent and polymer – polymer interactions in the dilute state were governed not only by the M_w and galactosyl substitution level but also by the chemical structure conformation of the polymer chains.

3.3. Steady state rheological behaviour

The flow behaviour curves for alfalfa gum dispersions in water at concentrations ranging from 0.1 to 2 % wt are illustrated at Fig. 4a. Except for the solution containing 0.1 % wt alfalfa gum, the flow curves indicated a predominant shear thinning behaviour ($n < 1$), which arises from the macromolecular re-orientation of the polymer chains on shear stress imposing. At very low shear rates, a Newtonian plateau was observed due to the ability of the disrupted polymer chain entanglements to be re-established. Fitting the Cross-Williamson model to the apparent viscosity – shear rate data, the zero-shear viscosity (η_0), the relaxation time (τ) and the critical shear rate at which the gum dispersions commence to behave as shear-thinning fluids ($\dot{\gamma}_{crit}$) were calculated (Table 3). As expected, the zero-shear rate and the critical shear rate values increased proportionally to the alfalfa gum concentration as the disruption predominates over the establishment of new polymer chain entanglements (Nwokocha, Williams, & Yadav, 2018; Sittikijyothin, Torres, & Gonçalves, 2005).

In Fig. 4b the plot of specific zero viscosity ($\eta_{sp} = \frac{\eta_0 - \eta_s}{\eta_s}$, where η_s = 0.89 mPa s) as function of the dimensionless coil overlap parameter (i.e. C[η]), is given. For most polysaccharides, the existence of two critical concentrations C* and C** is known to delimit the dilute, semi-dilute and entangled solution states (Sittikijyothin et al., 2005). For disordered polysaccharides e.g. dextran, alginates, hyaluronan etc., it has been shown that the intersection point of the dilute and semi-dilute solution states occurs at C[η] = 4 (Morris, Cutler, Ross-Murphy, Rees, & Price, 1981). Contrary to other random coil ordered polysaccharides, galactomannans exert a lower space occupancy i.e. C[η] = 0.8–3.0, which is generally attributed to the occurrence of specific intermolecular polymer interactions, a phenomenon known as hyperentanglement. According to the obtained master curve for the alfalfa gum dispersion (Fig. 4b), only the incipient overlap concentration C* = 0.306% wt was possible to be estimated. At C* the overlap coil concentration was ~ 2.9, which is similar to that of fenugreek and *Mimosa scabrella* gums (M/G ~ 1.0) (Doublier & Launay, 1981; Doyle, Lyons, & Morris, 2009; Ganter et al., 1992). In highly unsubstituted galactomannans (M/G ~ 2.0 or higher), hyperentanglement occurs via the non-specific association (towards the b crystallographic direction) of the galactosyl free regions ("smooth") of the mannan backbone (Morris et al., 1981). For highly substituted galactomannans (i.e. M/G ~ 1.0), the polymer interchain association via the b-axis direction is not sterically favoured. On the contrary, polymer interchain association occurs in the α-axis direction with the galactosyl groups lying above and under the mannan backbone (Doyle et al., 2009). Considering that the coil overlap parameter receives similar values for galactomannans of similar molecular structure conformation, it can be assumed that alfalfa and fenugreek gum share the same hyperentanglement mechanisms (C[η] at C* = 2.8 and 2.9, respectively).

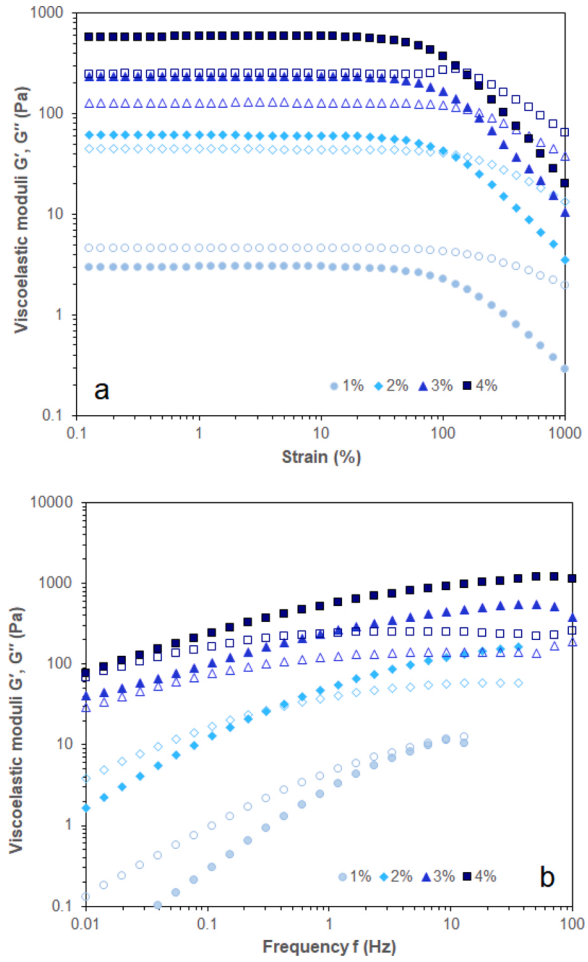

Fig. 5. Amplitude sweep (a) and frequency sweep (b) rheological spectra of alfalfa gum aqueous dispersions as a function of alfalfa gum concentration measured at 25 °C. The closed symbols denote the storage modulus (G′) whereas the open ones the loss modulus (G″).

According to the master curve (Fig. 4b), the specific viscosity dependence on alfalfa gum concentration ($\eta_{sp} = f(C[\eta]^b)$ was $\propto C^{2.3}$ and $C^{4.4}$ for the dilute and semi-dilute regimes, respectively. The obtained slope for the dilute regime appeared to be higher than the literature found values ($\propto C^{1.2}$ to $C^{1.7}$) for galactomannans (Gillet et al., 2017). However, upward deviations in the slopes for the dilute regime have been also reported for other galactomannans such as mesquite seed gum ($C^{2.2}$) (Yoo, Figueiredo, & Rao, 1994). On the other hand, the slopes for the semi-dilute regime are well within the range reported in the literature for galactomannans i.e. $\propto C^{3.3}$ to $C^{5.5}$ (Gillet et al., 2017) and almost identical to that of fenugreek gum i.e. $\propto C^{4.2}$ (Doyle et al., 2009). In Supplementary Fig. 1, the double logarithmic relationship between the viscosity (specific or apparent) and galactomannans concentration in the semi-dilute regime is given. In corroboration with the observations of Gillet et al. (2017), in the case of the η_{sp} – C[η] plots no clear relationships with M/G ratio and M_w were observed. On the other hand, the apparent viscosity exerted a reciprocal correlation ($r = 0.91$, $p < 0.001$) to the M_w, as expected.

3.4. Viscoelastic properties

Small amplitude oscillatory shear (SAOS) tests are considered as a standard methodology for assessing the structural and physical state of food colloids as influenced by processing and storage (Gunasekaran & Ak, 2000). To determine the boundary of linear viscoelastic (LVE) region of the alfalfa gum dispersions (1–4 % wt), amplitude sweeps (0.1–1,000

Table 4
Viscoelastic properties (strain sweeps with controlled shear deformation at 1 Hz and frequency sweeps (within the LVE regime) of the alfalfa gum dispersions (1 to 4% w/w, pH = 7) at 25 °C.

Alfalfa gum concentration (%)	Strain sweeps				Frequency sweeps			
	G'_{LVE} (Pa)	G''_{LVE} (Pa)	Yield stress, τ_y (Pa)	Flow point, τ_f (Pa)	G'_f (Pa)	Complex viscosity η^* (Pa s)	Crossover frequency f_c (Hz)	Slope G′ - ω
1	2.84 ± 0.19a	4.82 ± 0.24a	1.95 ± 0.12a	nd	nd	0.515 ± 0.02a	nd	0.921 ± 0.007d
2	56.6 ± 1.9b	44.9 ± 2.4b	27.5 ± 2.1b	58.5 ± 2.7a	40.3 ± 3.1a	7.47 ± 0.19b	0.41	0.671 ± 0.002c
3	220.5 ± 9.4c	130.6 ± 5.2c	102.4 ± 4.6c	257.5 ± 11.3b	108.4 ± 4.0b	35.3 ± 1.8c	nd	0.377 ± 0.002b
4	547.9 ± 25.2d	256.8 ± 4.3d	216.8 ± 12.8d	541.4 ± 12.7c	208.3 ± 10.1c	77.3 ± 2.7d	nd	0.356 ± 0.003a

[a–d] Different letters between the rows indicate significant difference ($p < 0.05$) according to Tukey's post hoc means comparison test; nd = not detected.

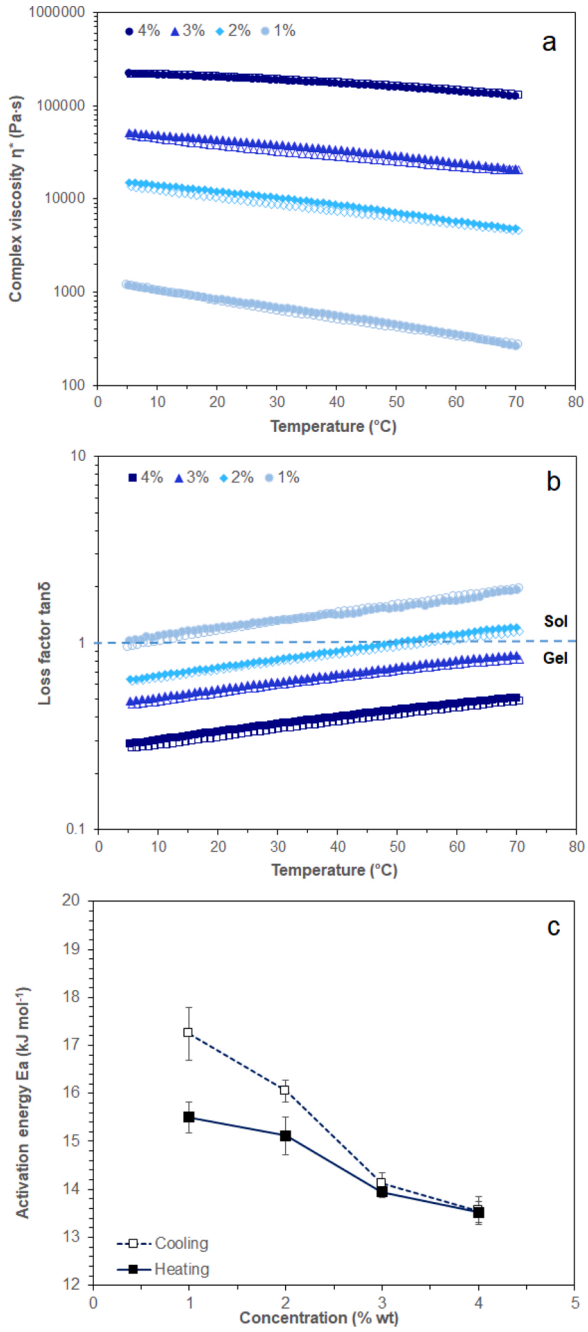

Fig. 6. Oscillatory thermo-rheological spectra of alfalfa gum dispersions measured in the LVE regime (1 Hz, 0.5% strain). (a): complex viscosity, (b) loss factor (stiffness) and (c) activation energies for cooling (closed symbols) and heating (open symbols) ramps as a function of alfalfa gum concentration.

% of strain) were performed (Fig. 5a). As illustrated in Fig. 5a, the strain boundary of the LVE regime was rather similar (i.e. 36.3–40.4 %) for all tested gum dispersions. However, the yield stress (τ_y) i.e. the minimum stress that is required to be imposed for inducing irreversible (plastic) deformation of the systems, exhibited a power-raw compliance to alfalfa gum concentration (Table 4).

The frequency sweep tests (Fig. 5b) were conducted within the LVR regime (strain 0.5 %) at 25 °C. As illustrated in Fig. 5b, the systems at ≤1 % wt of alfalfa gum exhibited a predominant viscous behaviour as $G'' < G'$ for the entire range of frequencies. At intermediate concentrations of alfalfa gum (i.e. $1 < c < 3$ % wt) a distinct viscoelastic behaviour with crossover points in the frequency range from 0.017 to 9.6 Hz was observed.

The crossover frequencies were reciprocally associated to the alfalfa gum concentration due to the increasing relaxation time as the polymer interchain associations becomes more evident (Sittikijyothin et al., 2005). At concentrations ≥ 3% wt, the aqueous alfalfa gum systems exhibited a dominant weak gel-like behaviour as $G' > G''$ and $0.6 < \tan\delta < 0.2$ for the entire range of frequencies. The slope of the double logarithmic G' - ω curves (Table 4), were reduced reciprocally to alfalfa gum confirming the formation of a gel-like polymer network. However, even at the highest gum concentration herein tested, the hydrogels did not achieve a true-gel conformational state (G' - ω slopes >> 0.1) (Rao, 2014).

The double logarithmic plot between the steady-state and dynamic rheological properties of alfalfa gum dispersions (1 and 2 % wt) was constructed in order to assess their compliance to the Cox-Merz superimposition rule. As displayed in Supplementary Fig. 2, the Cox-Merz empirical rule was closely obeyed at 1 % wt but a significant departure from superimposition was found at 2% wt. In general, disordered polysaccharides comply to the Cox-Merz rule when the entanglement of the polymer chains takes place via topological (non-specific) physical interactions. Corroborating our findings, it was shown in previous studies that semi-dilute galactomannan solutions (> 1 to 1.5 % wt) may deviate significantly from the superimposition particularly at low shear rates/frequencies (Nwokocha et al., 2018; Rincón, Muñoz, Ramírez, Galán, & Alfaro, 2014; Sittikijyothin et al., 2005). It has been demonstrated that the weak interchain association of galactomannans (or their aggregates) may exhibit diverse relaxation times under small deformation (η*) and steady state flow (η) conditions and therefore, the Cox-Merz rule is not satisfied (Gillet et al., 2017).

As illustrated in Fig. 6b, no sol-gel transitions were detected for the aqueous systems containing at least 3% wt of alfalfa gum, as the loss factor (tanδ) was lower than unity over the entire temperature range. However, both 3 and 4% alfalfa gum dispersions retained their weak gel-like character ($\tan\delta > 0.2$), even at very high temperature conditions. At lower gum concentrations, sol-gel transitions were observed to occur at $T_{sol\text{-}gel}$ = 5.2–9.5 and 49.6–54.5 °C for 1 and 2 % wt alfalfa gum dispersions, respectively. It should be noted that in both cases the upward temperature sweeps were associated with a shift of the sol-gel point to the right indicating that heating favoured (proportionally to the solvent availability) the hydrophobic interchain polymer bonding.

In the present study, non-isothermal kinetic modelling of complex viscosity as function of temperature was conducted. This allows getting a more pragmatic overview of the responsiveness of η* to dynamic temperature conditions e.g. throughout thermal food processing or dynamic food storage conditions. Due to the deviation from superimposition, the activation energy (E_a) values for η* were calculated for both cooling and heating steps. Parameters such as the M_w, the botanical origin, the ionic strength and the applied shear stress are known to impact the energy barrier to be overcome for initiating the flow of polysaccharide solutions. As seen in Fig. 6c, for alfalfa gum concentrations up to 3% wt, the E_a values were higher during the cooling step (E_a = 15.2 vs 14.5 kJ mol^{-1}), whereas the average E_a values (on increasing order of alfalfa gum content) were estimated at 13.5, 14.0, 15.1 and 15.5 kJ mol^{-1}. In general, the herein obtained E_a values are within the literature reported range for semi-dilute galactomannan dispersions i.e. 12–25 kJ mol^{-1} (Launay, Cuvelier, & Martinez-Reyes, 1997; Nwokocha, Senan, Williams, & Yadav, 2017). The elevated E_a values during the cooling process are primarily ascribed to the ability of the polymer hyperentangled networks to store the deformation energy (Razavi et al., 2018). Nevertheless, the reciprocal response of E_a values to gum concentration suggests that above a critical concentration (e.g. > 3 % wt) the dissipated or absorbed thermal energy cannot modify significantly the molecular mobility of the polymer chains.

4. Conclusions

A highly galactosyl substituted galactomannan of low protein residue (< 1.3% wt on dry basis) was wet extracted from the endosperm of alfalfa seeds. Sugar analysis revealed that the 99.2% of the total carbohydrate content was composed of mannose and galactose at a ratio of 1.18: 1. The alfalfa gum had an average molecular weight of 2×10^6Da, an intrinsic viscosity of 9.33 dL g^{-1} and a $\langle R_g \rangle_z$ of 48.4 nm. Despite its high degree of galactosyl substitution, alfalfa gum exhibited a low solvent (deionised water) affinity favouring the polymer – polymer chain interactions leading to the formation of larger polymer aggregates than other galactomannans of the similar M/G ratio, such as fenugreek gum. The critical dimensionless coil overlap concentration of alfalfa gum was 2.9 corresponding to a C* = 0.306 % wt. In line with other galactomannans, a steep slope ($\propto C^{4.2}$) of the η_{sp}– C[η] master curve branch corresponding to the semi-dilute regime was identified, most probably due to hyperentanglement i.e. occurrence of non-specific (—H bonding) polymer chain interactions. The latter explains also the departure of the semi-dilute alfalfa gum dispersions from the Cox-Merz superimposition rule. In the semi-dilute state, alfalfa gum dispersions exhibited a predominant viscous (C* < C ≤ 1 % wt) to viscoelastic character (1 ≤C ≤ 3% wt). Aqueous systems containing at least 3 % wt of alfalfa gum exerted a clear weak gel-like behaviour but without attaining a true gel state. Isothermal kinetic modelling of the viscoelastic properties in the LVE regime demonstrated that the temperature responsiveness of complex viscosity is reciprocally increased to alfalfa gum concentration. Alfalfa gum is a novel galactomannan of tremendous potential for the food industry due to its excellent thickening and gelling properties and the sustainable, ecologically versatile and economically resilient character of alfalfa plant.

CRediT authorship contribution statement

Thierry Hellebois: Conceptualization, Investigation, Formal analysis, Writing - original draft, Writing - review & editing. **Christos Soukoulis:** Conceptualization, Formal analysis, Writing - review & editing, Supervision, Project administration, Funding acquisition. **Xuan Xu:** Investigation, Writing - review & editing. **Jean-Francois Hausman:** Writing - review & editing, Project administration. **Alexander Shaplov:** Investigation, Writing - review & editing. **Petros S. Taoukis:** Writing - review & editing. **Claire Gaiani:** Writing - review & editing, Project administration, Supervision.

Acknowledgement

This work was supported by the Luxembourg Fonds National de la Recherche (Project PROCEED: CORE/2018/SR/12675439).

Appendix A. Supplementary data

Supplementary material related to this article can be found, in the online version, at doi:https://doi.org/10.1016/j.carbpol.2020.117394.

References

Bacenetti, J., Lovarelli, D., Tedesco, D., Pretolani, R., & Ferrante, V. (2018). Environmental impact assessment of alfalfa (Medicago sativa L.) hay production. *Science of the Total Environment, 635*, 551–558. https://doi.org/10.1016/j.scitotenv.2018.04.161

Ben-Othman, S., Jōudu, I., & Bhat, R. (2020). Bioactives from agri-food wastes: Present insights and future challenges. *Molecules, 25*(3), 510.

Boelt, B., Julier, B., Karagić, Đ., & Hampton, J. (2015). Legume seed production meeting market requirements and economic impacts. *Critical Reviews in Plant Sciences, 34*(1–3), 412–427. https://doi.org/10.1080/07352689.2014.898477

Bourbon, A. I., Pinheiro, A. C., Ribeiro, C., Miranda, C., Maia, J. M., Teixeira, J. A., et al. (2010). Characterization of galactomannans extracted from seeds of Gleditsia triacanthos and Sophora japonica through shear and extensional rheology: Comparison with guar gum and locust bean gum. *Food Hydrocolloids, 24*(2), 184–192.

Brummer, Y., Cui, W., & Wang, Q. (2003). Extraction, purification and physicochemical characterization of fenugreek gum. *Food Hydrocolloids, 17*(3), 229–236.

Chen, L., Liu, J., Zhang, Y., Dai, B., An, Y., & (Lucy) Yu, L. L. (2015). Structural, thermal, and anti-inflammatory properties of a novel pectic polysaccharide from Alfalfa (*Medicago sativa L.*) stem. *Journal of Agricultural and Food Chemistry, 63*(12), 3219–3228.

Chen, L., Liu, J., Zhang, Y., Niu, Y., Dai, B., & (Lucy) Yu, L. (2015). A novel alkaline hemicellulosic heteroxylan isolated from alfalfa (*Medicago sativa L.*) stem and its thermal and anti-inflammatory properties. *Journal of Agricultural and Food Chemistry, 63*(11), 2970–2978.

Cheng, Y., Brown, K. M., & Prud'homme, R. K. (2002). Preparation and characterization of molecular weight fractions of guar galactomannans using acid and enzymatic hydrolysis. *International Journal of Biological Macromolecules, 31*(1), 29–35.

Cornara, L., Xiao, J., & Burlando, B. (2016). Therapeutic potential of temperate forage legumes: A review. *Critical Reviews in Food Science and Nutrition, 56*(sup1), S149–S161.

Dhull, S. B., Sandhu, K. S., Punia, S., Kaur, M., Chawla, P., & Malik, A. (2020). Functional, thermal and rheological behavior of fenugreek (Trigonella foenum–graecum L.) gums from different cultivars: A comparative study. *International Journal of Biological Macromolecules, 159*, 406–414. https://doi.org/10.1016/j.ijbiomac.2020.05.094

Dobrenz, A. K., Smith, S. E., Poteet, D., & Miller, W. B. (1993). Carbohydrates in alfalfa seed developed for salt tolerance during germination. *Agronomy Journal, 85*(4), 834–836.

Doublier, J. L., & Launay, B. (1981). Rheology of galactomannan solutions: Comparative study of guar gum and locust bean gum. *Journal of Texture Studies, 12*(2), 151–172.

Doyle, J. P., Lyons, G., & Morris, E. R. (2009). New proposals on "hyperentanglement" of galactomannans: Solution viscosity of fenugreek gum under neutral and alkaline conditions. *Food Hydrocolloids, 23*(6), 1501–1510.

Gadkari, P. V., Tu, S., Chiyarda, K., Reaney, M. J. T., & Ghosh, S. (2018). Rheological characterization of fenugreek gum and comparison with other galactomannans. *International Journal of Biological Macromolecules, 119*, 486–495.

Ganter, J. L. M. S., Milas, M., Corrêa, J. B. C., Reicher, F., & Rinaudo, M. (1992). Study of solution properties of galactomannan from the seeds of *Mimosa scabrella*. *Carbohydrate Polymers, 17*(3), 171–175.

Gillet, S., Aguedo, M., Petrut, R., Olive, G., Anastas, P., Blecker, C., et al. (2017). Structure impact of two galactomannan fractions on their viscosity properties in dilute solution, unperturbed state and gel state. *International Journal of Biological Macromolecules, 96*, 550–559.

Grasdalen, H., & Painter, T. (1980). NMR studies of composition and sequence in legume-seed galactomannans. *Carbohydrate Research, 81*(1), 59–66.

Gunasekaran, S., & Ak, M. M. (2000). Dynamic oscillatory shear testing of foods — Selected applications. *Trends in Food Science & Technology, 11*(3), 115–127. https://doi.org/10.1016/S0924-2244(00)00058-3

Hojilla-Evangelista, M. P., Selling, G. W., Hatfield, R., & Digman, M. (2017). Extraction, composition, and functional properties of dried alfalfa (*Medicago sativa L.*) leaf protein. *Journal of the Science of Food and Agriculture, 97*(3), 882–888.

Jamir, K., Badithi, N., Venumadhav, K., & Seshagirirao, K. (2019). Characterization and comparative studies of galactomannans from *Bauhinia vahlii*, *Delonix elata*, and *Peltophorum pterocarpum*. *International Journal of Biological Macromolecules, 134*, 498–506.

Kontogiorgos, V. (2019). Galactomannans (Guar, Locust Bean, Fenugreek, Tara). In L. Melton, F. Shahidi, & P. Varelis (Eds.), *Encyclopedia of food chemistry* (pp. 109–113). Academic Press.

Launay, B., Cuvelier, G., & Martinez-Reyes, S. (1997). Viscosity of locust bean, guar and xanthan gum solutions in the Newtonian domain: a critical examination of the log (ηsp)o-log c[η]o master curves. *Carbohydrate Polymers, 34*(4), 385–395.

Liu, Y., Lei, F., He, L., Xu, W., & Jiang, J. (2020). Physicochemical characterization of galactomannans extracted from seeds of *Gleditsia sinensis Lam* and fenugreek. Comparison with commercial guar gum. *International Journal of Biological Macromolecules, 158*, 1047–1054.

Liu, Y., Xu, W., Lei, F., Li, P., & Jiang, J. (2019). Comparison and characterization of galactomannan at different developmental stages of *Gleditsia sinensis Lam*. *Carbohydrate Polymers, 223*, Article 115127.

López-Franco, Y. L., Cervantes-Montaño, C. I., Martínez-Robinson, K. G., Lizardi-Mendoza, J., & Robles-Ozuna, L. E. (2013). Physicochemical characterization and functional properties of galactomannans from mesquite seeds (*Prosopis spp.*). *Food Hydrocolloids, 30*(2), 656–660.

Marani, D., Hjelm, J., & Wandel, M. (2013). Use of intrinsic viscosity for evaluation of polymer-solvent affinity. *Annual Trans of the Nordic Rheology Society, 21*, 255–262.

Mathur, N. K. (2016). *Industrial galactomannan polysaccharides*. CRC Press.

McCleary, B. V., & Matheson, N. K. (1975). Galactomannan structure and β-mannanase and β-mannosidase activity in germinating legume seeds. *Phytochemistry, 14*(5), 1187–1194.

Mielmann, A. (2013). The utilisation of lucerne (*Medicago sativa*): a review. *British Food Journal, 115*(4), 590–600.

Moreira, A. S. P., Nunes, F. M., Domingues, M. R. M., & Coimbra, M. A. (2015). Chapter 19 - galactomannans in coffee. In V. R. Preedy (Ed.), *Coffee in health and disease prevention* (pp. 173–182). Academic Press.

Morris, E. R., Cutler, A. N., Ross-Murphy, S. B., Rees, D. A., & Price, J. (1981). Concentration and shear rate dependence of viscosity in random coil polysaccharide solutions. *Carbohydrate Polymers, 1*(1), 5–21.

Nwokocha, L. M., Senan, C., Williams, P. A., & Yadav, M. P. (2017). Characterisation and solution properties of a galactomannan from *Bauhinia monandra* seeds. *International Journal of Biological Macromolecules, 101*, 904–909.

Nwokocha, L. M., Williams, P. A., & Yadav, M. P. (2018). Physicochemical characterisation of the galactomannan from *Delonix regia* seed. *Food Hydrocolloids, 78*, 132–139.

Pajić, N., & Marković, T. (2016). Economic results in alfalfa seed production. *Ratarstvo i Povrtarstvo, 53*(3), 111–115. https://doi.org/10.5937/ratpov53-10851

Prajapati, V. D., Jani, G. K., Moradiya, N. G., Randeria, N. P., Nagar, B. J., Naikwadi, N. N., et al. (2013). Galactomannan: A versatile biodegradable seed polysaccharide. *International Journal of Biological Macromolecules, 60*, 83–92.

Qian, K. Y., Cui, S. W., Wu, Y., & Goff, H. D. (2012). Flaxseed gum from flaxseed hulls: Extraction, fractionation, and characterization. *Food Hydrocolloids, 28*(2), 275–283.

Rao, M. A. (2014). *Rheology of fluid, semisolid, and solid foods: Principles and applications* (3rd ed.). Springer US.

Razavi, S. M. A., Alghooneh, A., & Behrouzian, F. (2018). Thermo-rheology and thermodynamic analysis of binary biopolymer blend: A case study on sage seed gum-xanthan gum blends. *Food Hydrocolloids, 77*, 307–321.

Rincón, F., Muñoz, J., Ramírez, P., Galán, H., & Alfaro, M. C. (2014). Physicochemical and rheological characterization of *Prosopis juliflora* seed gum aqueous dispersions. *Food Hydrocolloids, 35*, 348–357.

Rodriguez-Canto, W., Chel-Guerrero, L., Fernandez, V. V. A., & Aguilar-Vega, M. (2019). *Delonix regia* galactomannan hydrolysates: Rheological behavior and physicochemical characterization. *Carbohydrate Polymers, 206*, 573–582.

Sciarini, L. S., Maldonado, F., Ribotta, P. D., Pérez, G. T., & León, A. E. (2009). Chemical composition and functional properties of *Gleditsia triacanthos* gum. *Food Hydrocolloids, 23*(2), 306–313.

Sittikijyothin, W., Torres, D., & Gonçalves, M. P. (2005). Modelling the rheological behaviour of galactomannan aqueous solutions. *Carbohydrate Polymers, 59*(3), 339–350.

Soukoulis, C., Gaiani, C., & Hoffmann, L. (2018). Plant seed mucilage as emerging biopolymer in food industry applications. *Current Opinion in Food Science, 22*, 28–42.

Wang, S., Dong, X., Ma, H., Cui, Y., & Tong, J. (2014). Purification, characterisation and protective effects of polysaccharides from alfalfa on hepatocytes. *Carbohydrate Polymers, 112*, 608–614.

Wang, S., Dong, X., & Tong, J. (2013). Optimization of enzyme-assisted extraction of polysaccharides from alfalfa and its antioxidant activity. *International Journal of Biological Macromolecules, 62*, 387–396.

Wei, Y., Lin, Y., Xie, R., Xu, Y., Yao, J., & Zhang, J. (2015). The flow behavior, thixotropy and dynamical viscoelasticity of fenugreek gum. *Journal of Food Engineering, 166*, 21–28.

Williams, P. A., & Phillips, G. O. (2009). 1 - Introduction to food hydrocolloids. In G. O. Phillips, & P. A. Williams (Eds.), *Handbook of hydrocolloids (second edition)* (pp. 1–22). Woodhead Publishing.

Wu, Y., Cui, W., Eskin, N. A. M., & Goff, H. D. (2009). Fractionation and partial characterization of non-pectic polysaccharides from yellow mustard mucilage. *Food Hydrocolloids, 23*(6), 1535–1541. https://doi.org/10.1016/j.foodhyd.2008.10.010

Yoo, B., Figueiredo, A. A., & Rao, M. A. (1994). Rheological properties of mesquite seed gum in steady and dynamic shear. *LWT - Food Science and Technology, 27*(2), 151–157.

Youssef, M. K., Wang, Q., Cui, S. W., & Barbut, S. (2009). Purification and partial physicochemical characteristics of protein free fenugreek gums. *Food Hydrocolloids, 23*(8), 2049–2053.